Cellular Effects and Antitumor Activity of RET Inhibitor RPI-1 on MEN2A-Associated Medullary Thyroid Carcinoma

Giuditta Cuccuru, Cinzia Lanzi, Giuliana Cassinelli, Graziella Pratesi, Monica Tortoreto, Giovanna Petrangolini, Ettore Seregni, Antonia Martinetti, Diletta Laccabue, Chiara Zanchi, Franco Zunino

Background: **The RET proto-oncogene encodes a receptor tyrosine kinase. RET oncogenes arise through sporadic and inherited gene mutations and are involved in the etiopathogenesis of medullary thyroid carcinoma, a cancer that responds poorly to conventional chemotherapy. Medullary thyroid carcinoma is a component of multiple endocrine neoplasia type 2 or MEN2 syndromes.** ***Methods:*** **We investigated the cellular effects of RPI-1, a novel 2-indolinone Ret tyrosine kinase inhibitor on cells that express RET C634 oncogenic mutants common in the MEN2A syndrome: NIH3T3 fibroblasts transfected with RET^{C634R} and human medullary thyroid carcinoma TT cells that express endogenous RET^{C634W}. RPI-1 antiproliferative activity was determined by cell proliferation and anchorage-independent growth assays. Expression and phosphorylation of Ret and of proteins involved in downstream signaling pathways were examined by immunoblotting. Antitumor activity of oral RPI-1 treatment was tested by using two dosing levels in nude mice bearing subcutaneous TT xenograft tumors. All statistical tests were two-sided.** ***Results:*** **The RPI-1 IC_{50} value for cell proliferation was 3.6 μM (95% confidence interval [CI] = 1.8 to 5.4 μM) in NIH3T3 cells expressing the Ret mutant compared with 16 μM (95% CI = 12.3 to 19.7 μM) in non-transfected NIH3T3 cells, and that for colony formation in soft agar was 2.4 μM (95% CI = 0.8 to 4.0 μM) and 26 μM (95% CI = 17 to 35 μM) in RET mutant–transfected and H-RAS-transfected NIH3T3 cells, respectively. In NIH3T3 cells expressing the Ret mutant, Ret protein and tyrosine phosphorylation were undetectable after 24 hours of RPI-1 treatment. In TT cells, RPI-1 inhibited proliferation, Ret tyrosine phosphorylation, Ret protein expression, and the activation of PLCγ, ERKs and AKT. In mice, oral daily RPI-1 treatment inhibited the tumor growth of TT xenografts by 81% ($P < .001$ versus control mice) and reduced the plasma levels of the specific biomarker calcitonin ($P = .01$ versus control mice). Twenty-five percent of RPI-1 -treated mice were tumor-free.** ***Conclusions:*** **Ret oncoproteins represent exploitable targets for therapeutic intervention in MEN2A-associated medullary thyroid carcinoma. The antitumor efficacy and oral bioavailability of RPI-1 support its therapeutic potential. [J Natl Cancer Inst 2004; 96:1006–14]**

Medullary thyroid carcinoma develops from the calcitonin-producing C cells of the thyroid gland *(1).* Medullary thyroid carcinoma may arise sporadically (75% of cases) or as a component of multiple endocrine neoplasia type 2 (MEN2) syndromes (25% of cases), which are autosomal dominant inherited diseases characterized by a strong predisposition to develop endocrine tumors. In the three clinical varieties of MEN2 syndromes identified, medullary thyroid carcinoma

Affiliations of authors: Preclinical Chemotherapy and Pharmacology Unit (G. Cuccuru, CL, G. Cassinelli, G. Pratesi, MT, G. Petrangolini, DL, CZ, FZ), and Nuclear Medicine Unit (ES, AM), Istituto Nazionale Tumori, Milan, Italy.

Correspondence to: Cinzia Lanzi, PhD, Department of Experimental Oncology, Preclinical Chemotherapy and Pharmacology Unit, Istituto Nazionale Tumori, via Venezian 1, 20133 Milan, Italy (e-mail: cinzia.lanzi@istitutotumori.mi.it).

See "Notes" following "References."

DOI: 10.1093/jnci/djh184

represents the main prognostic factor. In the most frequent MEN2 subtype, MEN2A, medullary thyroid carcinoma is associated with pheocromocytoma in approximately 50% of affected individuals and hyperparathyroidism in approximately 20% of affected individuals. In the subtype MEN2B, medullary thyroid carcinoma is associated with pheocromocytoma (in 50% of affected individuals), enteric ganglioneuromas, and skeletal and ocular abnormalities. The least common hereditary form of medullary thyroid carcinoma is the familial variant (familial medullary thyroid carcinoma), in which medullary thyroid carcinoma is the only phenotype *(2)*. The treatment of choice for both sporadic and hereditary medullary thyroid carcinoma is surgery *(3)*. Recurrences are observed in approximately 50% of patients, and the prognosis for unresectable or metastatic medullary thyroid carcinoma is poor because radiation therapy and chemotherapy regimens have only a limited palliative role *(3,4)*.

Ret receptor tyrosine kinase is frequently aberrantly activated in thyroid tumors. Several lines of evidence suggest that it might represent a useful target for specific therapeutic approaches. Oncogenic activation of the RET gene is recognized as an early pathogenic event in papillary and medullary thyroid carcinomas. In papillary carcinoma, the most frequent thyroid malignancy, somatic rearrangements of the RET gene that generate oncogenic fusion proteins are found in approximately 30% of the cases *(5,6)*. Somatically arising RET point mutations are present in about 50% of sporadic medullary thyroid carcinoma cases. The finding that germline missense mutations are present in virtually all families with MEN2 syndromes led to the implementation of early genetic screening as the standard for diagnosing MEN2 syndromes *(7)*. The clinical relevance of RET in thyroid cancer is further strengthened by evidence that genetically engineered mice expressing thyroid-targeted RET oncogenes develop thyroid tumors that mimic human tumor phenotypes *(8,9)*.

The RET proto-oncogene is characterized by the presence of cadherin-related motifs and a cysteine-rich domain in the extracellular domain. Two major Ret isoforms of 1072 (short) or 1114 (long) amino acids are generated by alternative splicing *(10)* and posttranslational glycosylation *(11)*. Partially and fully glycosylated forms of Ret, the precursors and mature forms of the receptor, are expressed in the endoplasmic reticulum and at the cell surface, respectively *(12)*. Activation of the wild-type Ret receptor requires interaction with a ligand belonging to the glial cell line–derived neurotrophic factor (GDNF) family, which induces the subsequent autophosphorylation of Ret. As in the case of other receptor tyrosine kinases, specific phosphorylated tyrosine residues represent the docking sites for molecules containing SH2 or phosphotyrosine-binding (PTB) domains. The recruitment of multiprotein complexes, in turn, elicits downstream signaling events involving Ras/ERK (extracellular signal-regulated kinase), PI3K/AKT, and phospholipase Cγ (PLCγ)–dependent pathways *(6,10)*.

Dominant gain-of-function mutations of the RET gene found in human tumors generate ligand-independent, constitutively active tyrosine kinase oncoproteins that are able to transform NIH3T3 fibroblasts *(5,13–15)*. The mechanism of oncogenic activation varies among different RET mutants. In MEN2A patients, Ret mutations occur in the extracellular, cysteine-rich domain at cysteine residues 609, 611, 618, 620, 630, or 634 (C634 mutants are found in approximately 87% of MEN2A patients) and result in the substitution of another amino acid in place of the cysteine. In the wild-type Ret protein, these cysteines are connected by intramolecular disulfide bonds. Their loss by mutation may result in the formation of intermolecular bonds through partner cysteine residues of other Ret mutants, thereby inducing Ret activation by covalent dimerization *(7,16)*.

The constitutive tyrosine kinase activity of Ret oncoproteins suggests the possibility of using small-molecule inhibitors to block their transforming signaling *(17)*. In previous studies, we showed that the small molecule inhibitor arylidene-2-indolinone RPI-1 can inhibit the product of RET/papillary thyroid carcinoma-1 (PTC1), the most frequent RET oncogene found in sporadic papillary thyroid carcinomas *(6)*. RPI-1 abolished the constitutive tyrosine phosphorylation of the Ret/ptc1 oncoprotein and its signaling in NIH3T3 mouse fibroblasts transfected with RET/PTC1 and in human papillary thyroid carcinoma cells spontaneously expressing the RET/PTC1 rearrangement *(18,19)*. These findings prompted us to investigate the effects of RPI-1 in cells carrying medullary thyroid carcinoma-associated RET mutations. In this study, we examined the cellular and biochemical effects of RPI-1 treatment on cells containing constitutively active Ret via mutation of C634. Specifically, our cellular models included NIH3T3 fibroblasts transfected with a RET mutant carrying the C634R substitution (RET^{C634R}), which is found in more than 50% of MEN2A patients, and the human medullary thyroid carcinoma cell line TT, which spontaneously expresses another MEN2A-associated RET mutant, RET^{C634W}. In addition, we investigated the ability of RPI-1 to inhibit the *in vivo* growth of TT tumor xenografts.

Materials and Methods

Drug Treatment and Cell Culture

The synthesis and chemical structure of RPI-1 (1,3-dihydro-5,6-dimethoxy-3-[(4-hydrophenyl)methylene]1-H-indol-2-one) have been reported previously *(18)*. For *in vitro* experiments, an RPI-1 stock solution was prepared in 100% dimethylsulfoxide (DMSO). RPI-1 and DMSO (control) were diluted in culture medium for use (final concentration of solvent = 0.5% DMSO, vol/vol). For *in vivo* studies, solid RPI-1 was dissolved in absolute ethanol and Cremophor EL (each 5% of the final volume). The solution was stirred at 4 °C until clear and maintained at 4 °C for 12–24 hours. Just before use, it was diluted by slowly adding cold 0.9% NaCl solution (90% of the final volume) while stirring. During and after dilution, the RPI-1 solution remained on ice. The final RPI-1 concentration was 3.3 mg/mL (maximum concentration allowed before precipitation).

$NIH3T3^{MEN2A}$ and $NIH3T3^{H\text{-}RAS}$ cells are NIH3T3 mouse fibroblasts transfected with the C634R mutant of RET (RET^{C634R} short isoform) or H-RAS oncogenes, respectively *(20)*. Both transfected cell lines were routinely maintained at 37 °C in a 10% CO_2 atmosphere in Dulbecco's modified Eagle Medium (DMEM; BioWhittaker, Verviers, Belgium) supplemented with 5% calf serum (Colorado Serum Company, Denver, CO). Untransfected NIH3T3 cells were cultured in DMEM containing 10% calf serum. The human TT cell line was derived from a metastatic medullary thyroid carcinoma harboring a

MEN2A-type RET mutation, specifically, a cysteine-to-tryptophan substitution at codon 634 (C634W) *(21,22)*. TT cells were subcultured in Ham's F12 medium (BioWhittaker) supplemented with 15% fetal bovine serum (Life Technologies, Gaithersburg, MD) and were maintained at 37 °C in a 5% CO_2 atmosphere.

Cell Growth Assays

Cell sensitivity to RPI-1 was assessed by cell growth and anchorage-independent growth inhibition assays. To measure cell proliferation, exponentially growing cells were seeded in duplicate on six-well plates at 2500–10 000 cells per square centimeter and treated with RPI-1 or DMSO alone, after at least one round of cell division (96 hours for TT cells and 24 hours for the NIH3T3 transfectants). After 3 or 7 days of drug exposure, cells were harvested by trypsin treatment and counted directly with a Coulter counter (Coulter Electronics, Luton, U.K.). Alternatively, TT cells were seeded in octuplicate on 96-well plates at 10 000 cells per square centimeter, treated with RPI-1 or DMSO, and then subjected to the sulforhodamine B colorimetric assay *(23)* at different time points over a period of 21 days. The anchorage-independent growth assay was performed as previously described *(18)*. Briefly, a cell suspension (15 000 cells per milliliter) in medium containing 0.33% agarose (Sigma Chemical Company, St. Louis, MO) and the appropriate concentration of RPI-1 or vehicle (DMSO) was layered onto semisolid agarose (0.5% agarose in medium) in duplicate on 9.6-cm^2 dishes. After 8–10 days of incubation at 37 °C, cell colonies were stained with *p*-iodonitrotetrazolium violet (Sigma), visualized with a magnifying projector, and counted. In both assays, the RPI-1 IC_{50} values (drug concentrations producing 50% inhibition) were calculated from the dose–response curves obtained with Microcal Origin, version 4.10 (Microcal Software, Northampton, MA). Each experiment was performed 3–4 times.

Immunoprecipitation and Western Blot Analysis

For immunoblots performed with whole-cell extracts, samples were prepared after treatment by lysing cells in sodium dodecyl sulfate (SDS) sample buffer (62.5 m*M* Tris–HCl [pH 6.8], 2% SDS) containing 1 m*M* phenylmethylsulfonyl fluoride, 10 μg/mL pepstatin, 12.5 μg/mL leupeptin, 2 μg/mL aprotinin, 1 m*M* sodium orthovanadate, and 1 m*M* sodium molybdate. Protein concentration was determined using the bicinchoninic acid (BCA) method (Pierce, Rockford, IL). Samples were then prepared for electrophoresis by adding 10% glycerol, 5% β-mercaptoethanol, and 0.001% bromophenol blue.

For immunoprecipitation experiments, cells were treated with RPI-1 or DMSO for 24 hours. Cell monolayers were rinsed twice with cold phosphate-buffered saline (137 m*M* NaCl, 1.76 m*M* KH_2PO_4, 2.7 m*M* KCl, 8.1 m*M* Na_2HPO_4 [pH 7.4]) supplemented with 0.1 m*M* sodium orthovanadate and incubated on ice for 20 minutes in lysis buffer (50 m*M* HEPES [pH 7.6], 150 m*M* NaCl, 10% glycerol, 1% Triton X-100, 1.5 m*M* $MgCl_2$, 1 m*M* EGTA, 100 m*M* NaF, 10 m*M* sodium pyrophosphate, and four protease inhibitors—10 μg/mL antipain, 20 μg/mL chymostatin, 10 μg/mL E64, and 1 mg/mL Pefabloc SC). Cells were collected by scraping, pushed through a 22-gauge needle, and centrifuged at 10 000*g*, for 20 minutes at 4 °C. Supernatants (cell extracts) were collected, and protein concentration was determined by the BCA reaction. Cell extracts (0.5–5 mg) were immediately incubated with pre-swelled protein A–agarose resin (Sigma) and the indicated antibody for 2 hours at 4 °C with rotation. For each milligram of cell extract, 18 μg of anti-Ret *(24)* or 4 μg of anti-PLC γ (Santa Cruz Biotechnology, Santa Cruz, CA) were used. After washing the resin three times with 20 m*M* HEPES (pH 7.6), 150 m*M* NaCl, 10% glycerol, and 0.1% Triton X-100, the immunoprecipitates were eluted with complete sample buffer (SDS sample buffer containing 10% glycerol, 5% β-mercaptoethanol, and 0.001% bromophenol blue).

Immunoprecipitates or whole-cell lysates (30–60 μg) were resolved by SDS–polyacrylamide gel electrophoresis (7.5% or 10% acrylamide wt/vol) and electrophoretically transferred to nitrocellulose filters. Nonspecific binding was blocked by incubating membranes in 1% bovine serum albumin, 3% ovalbumin (wt/vol) in TBS-T (25 m*M* Tris–HCl [pH 7.2], 150 m*M* NaCl, and 0.1% Tween 20) for 1 hour at room temperature. Membranes were then incubated with primary antibodies in TBS-T overnight at 4 °C. Immunoreactive bands were visualized with enhanced chemiluminescence detection systems from Pierce or Amersham Biosciences (Little Chalfont, U.K.) after incubating membranes with horseradish peroxidase–conjugated anti-mouse or anti-rabbit secondary antibodies (Amersham Biosciences). When needed, membranes were stripped with 2% SDS, 62.5 m*M* Tris–HCl [pH 6.8], and 0.7% β-mercaptoethanol for 30 minutes at 45 °C and re-probed as described above.

The following primary rabbit polyclonal antibodies were used: anti-Ret, which recognizes a carboxy-terminal sequence (amino acids 1000–1014) common to the short and long Ret isoforms *(24);* anti-pY1062-Ret, which recognizes the Y1062-phosphorylated Ret *(25);* anti-pAkt, which recognizes the phosphorylated S473 of Akt (Cell Signaling Technology, Beverly, MA); anti-p44/42 ERKs (Upstate Biotechnology, Lake Placid, NY); anti-PLCγ (Santa Cruz Biotechnology, Santa Cruz, CA); and anti-actin (Sigma). The monoclonal antibodies were anti-pTyr antibody clone 4G10 (Upstate Biotechnology), which recognizes phosphorylated tyrosine residues; anti-PKBα/Akt (Transduction Laboratories, Lexington, KY); and anti-phospho-p44/42 ERKs (pERKs) (Thr202/Tyr204), which recognize ERKs that are doubly phosphorylated at these residues (Cell Signaling Technology).

In Vivo Studies

All *in vivo* experiments were performed using 8- to 11-week-old female athymic nude CD-1 mice (Charles River, Calco, Italy). Mice were maintained in laminar flow rooms with constant temperature and humidity. Experimental protocols were approved by the Ethics Committee for Animal Experimentation of the Istituto Nazionale Tumori (Milan, Italy), according to the United Kingdom Coordinating Committee on Cancer Research Guidelines *(26)*.

Human medullary thyroid carcinoma TT cells (1.6×10^7 cells in suspension) were inoculated subcutaneously into the right flank of mice. Each control or RPI-1-treated group included 8–10 tumors (one tumor per mouse). TT cells were injected on day 0, and tumor growth was followed by biweekly tumor diameter measurements using a vernier caliper. Tumor weight was calculated, considering tumor density equal to 1, according to the following formula: tumor weight (mg) = tumor volume

(mm^3) = $d^2 \times D/2$, where d and D are the shortest and the longest diameter, respectively. RPI-1 treatment started when tumors were just measurable (mean tumor weight was ≈50 mg), at approximately 25 days after tumor cell inoculation. RPI-1 was delivered orally twice a day for 10 or 40 days. The drug was administered in a volume of 15–30 mL/kg of body weight. Control mice were treated with vehicle (ethanol, Cremophor EL, 0.9% NaCl solution at 5 : 5 : 90) in parallel with mice treated with RPI-1.

Drug efficacy was assessed either as mean percentage of tumor weight inhibition in drug-treated versus control mice (expressed as tumor weight inhibition percent = 100 – [mean tumor weight of treated mice/mean tumor weight of control mice × 100]), evaluated during and after drug treatment, or as "cure," that is, no evidence of tumor at the end of the experiments. Experimental groups were sacrificed by cervical dislocation when mean tumor weight was at a maximum of 2.0 ± 0.5 g.

RPI-1 tolerability was assessed in tumor-bearing mice as either lethal toxicity (i.e., any death in treated mice occurring before any control death) or percent body weight loss (body weight loss percent = 100 – [body weight on day *x*/body weight on day 1 × 100], where *x* represents 1 day after or during the treatment period). The maximum body weight loss values are reported.

Calcitonin Assay

Control and RPI-1-treated mice were bled under general anesthesia by venous orbital puncture. For anesthesia, a solution of ketamine (Ketavet 50; Farmaceutici Gellini, Aprilia, Italy), xylazine (Rompun; Bayer, Leverkusen, Germany) and saline (at a ratio of 20 : 2.5 : 77.5) was prepared and delivered intraperitoneally at a dose of 10 mL/kg of body weight. Blood samples were centrifuged (4000*g* for 10 minutes), and the plasma (supernatant) was frozen until analysis. All procedures were performed on ice to prevent the enzymatic degradation of calcitonin. Calcitonin levels in plasma were measured with an immunoradiometric assay (IRMA) kit (Calcitonin Assay; Scantibodies Laboratory, Santee, CA), with two different anti-human calcitonin goat polyclonal antibodies, according to the manufacturer's instructions.

Statistical Analysis

Student's *t* test (two-tailed) was used to compare tumor weight and calcitonin levels in control and RPI-1-treated mice. The Spearman rank correlation analysis *(27)* was used to determine the relationship between tumor weight and calcitonin levels.

RESULTS

Effects of RPI-1 on NIH3T3 Cells Transfected With RET^{C634R}

We investigated the effects of RPI-1 in NIH3T3 fibroblasts stably transfected to express the RET mutant C634R (RET^{C634R}). The effect of RPI-1 on the proliferation of these cells was examined by counting cells after 72 hours of RPI-1 treatment. As shown in Table 1, NIH3T3 cells transfected with the RET^{C634R} mutant ($NIH3T3^{MEN2A}$) were nearly four times more sensitive to the growth inhibitory effects of RPI-1 than

Table 1. IC_{50} values for antiproliferative effects of RPI-1 on NIH3T3 cells and NIH3T3 cells transformed by the MEN2A-RET (C634R) or H-RAS oncogenes*

Cell line	Cell proliferation (95% CI)†	Colony formation (95% CI)‡
NIH3T3	16.0 (12.3 to 19.7)	—
$NIH3T3^{H\text{-}RAS}$	14.1 (8.0 to 20.2)	26 (17 to 35)
$NIH3T3^{MEN2A}$	3.6 (1.8 to 5.4)	2.4 (0.8 to 4.0)

*IC_{50} (μM) indicates RPI-1 concentration required to inhibit cell proliferation or colony formation by 50%, following treatment. Mean of 3–4 independent experiments, each performed in duplicate, with 95% confidence intervals (CIs).

†After 72 hours of treatment.

‡After 8 days of treatment; — = NIH3T3 fibroblasts do not form colonies in soft agar.

NIH3T3 cells transfected with H-RAS ($NIH3T3^{H\text{-}RAS}$) or than parental NIH3T3 cells. The selectivity of RPI-1 for RET^{C634R}-expressing cells was higher in the soft agar assay. In this assay, the growth of $NIH3T3^{MEN2A}$ colonies was 10 times more sensitive to RPI-1 than that of $NIH3T3^{H\text{-}RAS}$ colonies.

Under normal conditions, tyrosine residues of wild-type Ret are phosphorylated upon ligand stimulation. In contrast, a constitutive ligand-independent tyrosine phosphorylation is a feature of the oncogenic forms of Ret *(6,10,28)*. To examine the phosphorylation status of the Ret mutant receptor expressed in treated $NIH3T3^{MEN2A}$ transfectants, cell lysates were prepared after treatment with 10 μM RPI-1 for various times (2, 24, 48, or 72 hours). Ret expression and tyrosine autophosphorylation were analyzed by western blotting. As shown in Fig. 1, A, inhibition of Ret tyrosine phosphorylation was evident within 2

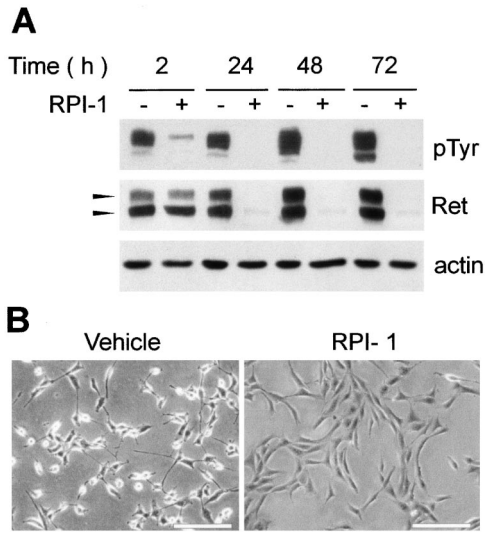

Fig. 1. Effects of RPI-1 on $NIH3T3^{MEN2A}$ cells. **A**) Ret autophosphorylation and expression. Whole cell lysates were prepared from $NIH3T3^{MEN2A}$ cells exposed to vehicle (dimethylsulfoxide) (–) or 10 μM RPI-1 (+) for the indicated times. Equal amounts of protein from each sample were separated by sodium dodecyl sulfate–polyacrylamide gel electrophoresis, transferred to nitrocellulose membranes, and subjected to western blotting with an anti-phosphotyrosine (pTyr) antibody. Ret expression was detected after stripping and re-probing the filter with anti-Ret antibody. **Arrowheads** indicate the 170- and 150-kd species of Ret, which differ in extent of glycosylation. The blot was probed with anti-actin antibodies as a control for equal protein loading. **B**) Reversion of the transformed morphologic cell phenotype. Cells treated with vehicle or 10 μM RPI-1 for 24 hours were photographed under a phase-contrast microscope. **Scale bars** = 200 μm. Representative results of at least two independent experiments are shown.

hours of RPI-1 treatment. After prolonged RPI-1 treatment (24–72 hours), the disappearance of tyrosine phosphorylation was associated with lowered expression of both the fully glycosylated mature Ret (170 kd) and the partially glycosylated precursor (150 kd).

Consistent with its ability to inhibit the transforming properties of Ret mutants *(18)*, RPI-1 induced a reversion of the typical transformed morphologic phenotype of NIH3T3^{MEN2A} cells. RPI-1-treated cells appeared more flattened and ordered than control DMSO-treated cells (Fig. 1, B). In contrast, no effect of RPI-1 on NIH3T3$^{H\text{-}RAS}$ cellular morphology was observed (data not shown).

Effects of RPI-1 on Human TT Medullary Thyroid Carcinoma Cells

The effects of RPI-1 treatment were further investigated in a human medullary thyroid carcinoma cell line, known as TT, that naturally expresses the RET^{C634W} mutant *(21,22)*. Because of their slow doubling time (4 days), TT cells were monitored for up to 21 days in the presence of RPI-1. Dose-dependent inhibition of TT cell proliferation was evident, with a growth arrest at drug concentrations higher than 10 μM (Fig. 2). After 7 days of treatment, the RPI-1 IC_{50} was 7.2 μM (95% confidence interval = 6.6 to 7.8 μM). Experiments in which we replaced medium and treatment drugs once a week gave similar results to those above (data not shown).

We then investigated the effects of RPI-1 on Ret activation and signaling in TT cells. After treatment with three concentrations of RPI-1 (7, 20, and 60 μM) for 24 hours, cells were lysed, Ret protein was immunoprecipitated with anti-Ret antibody, and the resulting immunocomplexes were probed with an anti-pTyr antibody. As Fig. 3, A, shows, we observed a dose-dependent

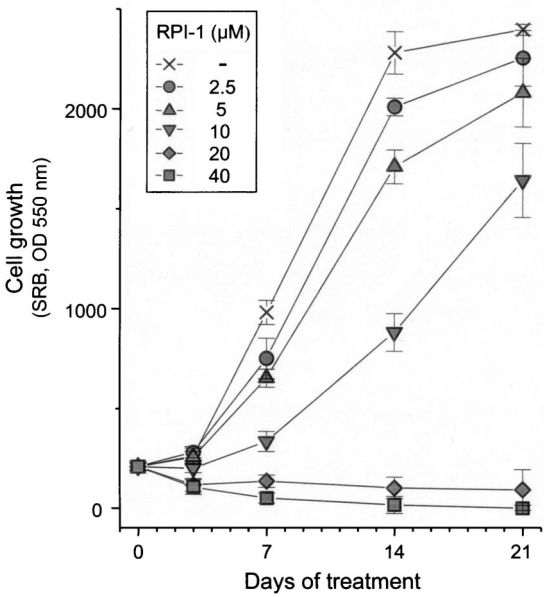

Fig. 2. Effect of RPI-1 on growth of TT cells. Cells were seeded in 96-well plates. After 96 hours, vehicle (dimethylsulfoxide) (×) or RPI-1 at the indicated concentrations was added to the medium, and cell growth was measured over a period of 21 days by the sulforhodamine B (SRB) colorimetric assay. Cell density is expressed as optical density (OD) units at 550 nm. One representative experiment of three independent experiments is shown. Each point represents the mean of eight independent replicates. **Error bars** represent the 95% confidence intervals.

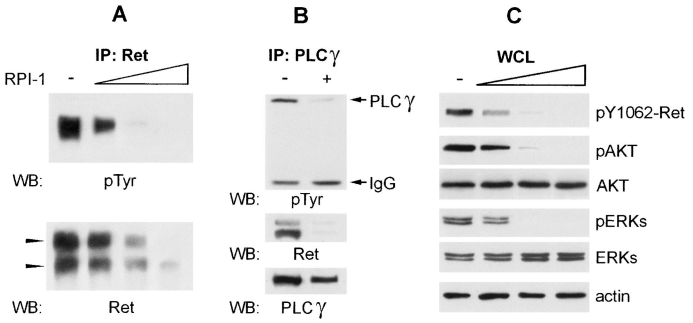

Fig. 3. Effect of RPI-1 on Ret activation and signaling in human TT cells. **A**) Ret autophosphorylation. TT cells were treated with dimethylsulfoxide (–) or increasing concentrations of RPI-1 (7, 20, 60 μM) for 24 hours. TT cell lysates containing equal amounts of protein were immunoprecipitated (IP) with an anti-Ret antibody. Immunoprecipitates were separated by sodium dodecyl sulfate–polyacrylamide gel electrophoresis, transferred to nitrocellulose membranes, and subjected to western blotting (WB) with an anti-phosphotyrosine (pTyr) antibody. To detect Ret expression, the filter was stripped and re-probed with anti-Ret antibody. **Arrowheads** indicate the 170- and 150-kd differentially glycosylated species of Ret. **B**) Phospholipase Cγ (PLCγ) tyrosine phosphorylation and interaction with Ret. TT cells were exposed to dimethylsulfoxide (–) or 20 μM RPI-1 (+) for 24 hours. Equal amounts of protein were immunoprecipitated (IP) with anti-PLCγ antibody. Immunoprecipitates were resolved by sodium dodecyl sulfate–polyacrylamide gel electrophoresis and transferred to nitrocellulose filters for western blot analysis with anti-phosphotyrosine, anti-Ret, or anti-PLCγ antibodies. **C**) Effects of RPI-1 on Ret-dependent pathways. Cells were treated with RPI-1 as in (**A**). Whole cell lysates (WCL) were prepared, and equal amounts of proteins from each sample were separated by sodium dodecyl sulfate–polyacrylamide gel electrophoresis and processed for western blotting. The main Ret docking site was detected by the phospho-specific antibody anti-pY1062-Ret. Downstream pathways were analyzed by probing the membranes with the phosphorylation-specific antibodies anti-phospho-Akt Ser^{473} (pAKT) and anti-phospho-p44/42 extracellular signal-regulated kinase Thr^{202}/Tyr^{204} (pERK). Blots were then stripped and re-probed with antibodies directed against the respective proteins (AKT and ERK). Actin is shown as a control for equal protein loading. Representative results of at least two independent experiments are shown.

inhibition of both Ret expression and tyrosine phosphorylation, in agreement with the effect observed in NIH3T3^{MEN2A} transfectants (Fig. 1, A).

Deregulated signaling occurs when SH2- and PTB-containing proteins are constitutively bound to phosphorylated tyrosine residues on Ret oncoproteins *(6,10)*. Specifically, Ret oncoproteins, including MEN2A-type C634 mutant receptors, bind constitutively to PLCγ through the phosphorylated Y1015 docking site *(24,28)*. The results of co-immunoprecipitation experiments showed that RPI-1 treatment (20 μM for 24 hours) strongly reduced the binding of Ret to PLCγ (Fig. 3, B). In addition, tyrosine phosphorylation of PLCγ was reduced in treated cells (Fig. 3, B).

Next, we examined the effect of RPI-1 on the phosphorylation status of the multifunctional docking site pY1062 of Ret, which is considered crucial for the transforming activity of MEN2A-type C634 mutant Ret receptors and other Ret oncoproteins *(29)*. Whole-cell lysates prepared from TT cells treated with increasing concentrations of RPI-1 (7, 20, and 60 μM) for 24 hours were analyzed by western blotting with a phospho-specific anti-pY1062-Ret antibody. Like overall Ret tyrosine phosphorylation (Fig. 3, A), pY1062 disappeared with increasing RPI-1 dose (Fig. 3, C). The pY1062 docking site has been implicated in the activation of Ras/ERK and PI3K/AKT pathways by either ligand-activated or oncogenic Ret proteins *(30,31)*. Thus, we examined the phosphorylation status of ERKs

Table 2. Antitumor activity of oral RPI-1 against the human TT MEN2A-associated medullary thyroid carcinoma xenograft

Experiment	Daily RPI-1dose, mg/kg	Days of treatment*	Mean tumor weight, mg (95% CI)†	Tumor weight inhibition, %†	Cures‡	Maximum body weight loss, %§	Toxic deaths
A	vehicle	25–34	244 (181 to 308)		0/9	4	0/9
A	2 × 50	25–34	98 (53 to 144)	60	0/8	4	0/8
A	2 × 100	25–34	60 (19 to 101)	75	2/8	7	0/8
B	vehicle	27–66	580 (381 to 779)		0/10	0	0/10
B	2 × 100	27–66	113 (35 to 191)	81	2/8	2	0/8

*Treatment was started when mean tumor weight was approximately 50 mg; RPI-1 or vehicle was delivered daily by gavage, twice a day, at the indicated days. CI = confidence interval.

†Tumor weights were determined on day 39 after tumor inoculation for experiment A and on day 66 for experiment B. Tumor weight inhibition percent = 100 − (mean tumor weight of treated mice/mean tumor weight of control mice × 100).

‡Tumor-free mice/total number of mice in the group at the end of experiments. Day 53 was the end of experiment A. In experiment B, cures were achieved by day 53 and lasted up to the end of the experiment at day 140.

§Maximum body weight loss percent = 100 − (body weight on day *x*/body weight on day 1 × 100), where *x* represents a day during or a day after the treatment period.

and AKT in control and RPI-1-treated TT cells by western blot analysis with antibodies that specifically recognize the phosphorylated (i.e., activated) forms of these proteins. Fig. 3, C, shows that phosphorylation, and hence activation, of ERKs and AKT was inhibited by RPI-1 in a dose-dependent manner, similar to that observed for Ret inhibition (Fig. 3, A).

Effects on Human TT Medullary Thyroid Carcinoma Xenografts

The antitumor efficacy of RPI-1 was investigated in mice carrying subcutaneous xenograft tumors of human medullary thyroid carcinoma TT cells (Table 2). Two daily RPI-1 dose levels (each fractionated in two oral administrations) were investigated. This schedule was chosen to allow continuous exposure of tumor cells to the drug. A dose-dependent effect on tumor growth was observed, with a dose of 2 × 50 mg/kg/day resulting in less tumor weight inhibition than the 2 × 100 mg/kg/day dose after 10 days of treatment ($P = .003$ and $P < .001$, versus controls, respectively, by two-sided Student's *t* test). Moreover, in the group receiving the highest dose, two of eight mice were tumor-free at the end of the experiment (day 53) (Table 2, experiment A). An improved antitumor effect, without evidence of toxicity, was achieved by a more prolonged RPI-1 administration of 2 × 100 mg/kg/day, which was well-tolerated for up to 40 days (maximum time investigated) in terms of body weight loss and lethal toxicity (Table 2, experiment B). The inhibitory effect of the drug was observed immediately, and tumor growth was maintained under control for the treatment period, reaching a tumor weight inhibition of 81% relative to that in controls ($P < .001$) at the end of treatment (day 66). Approximately 2 months after the interruption of treatment (day 110), treated tumors were still statistically significantly smaller than control tumors (tumor weight inhibition = 52%; $P = .01$), and two of eight mice were still tumor-free at the end of the experiment (day 140). In these two mice, tumors had disappeared during treatment, at approximately day 50. The growth curves of the two experiments summarized in Table 2 are shown in Fig. 4 (mean values from 8–10 mice per point). Because of drug solubility and formulation limitations, higher doses were not tested.

Because thyroid C cells secrete the polypeptide hormone calcitonin, which serves as a specific medullary thyroid carcinoma biomarker in the clinic *(4)*, plasma levels of calcitonin were assessed in control and treated mice at different times during the experiments. When plasma calcitonin values were plotted against tumor weights (Fig. 5, A), a strong linear relationship was found ($r = .95$, $P < .001$, by Spearman rank correlation test). As shown in Fig. 5, B, the calcitonin plasma levels

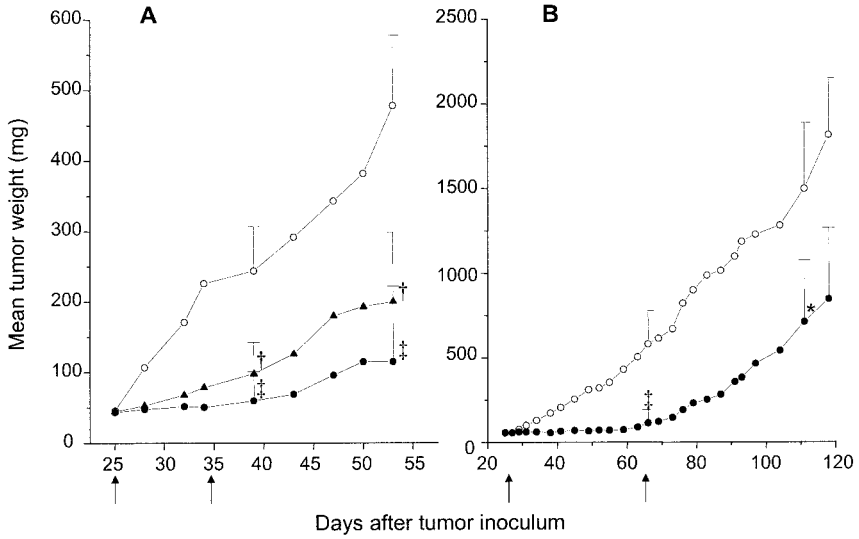

Fig. 4. Effect of RPI-1 on human TT tumor xenograft growth. TT cells (1.6×10^7) were subcutaneously inoculated into the right flank of nude mice. Tumor weight was assessed twice a week. When tumor weights were approximately 50 mg, mice were treated orally twice daily with RPI-1 for different times. **A**) TT tumor-bearing mice were treated for 10 days from day 25 to day 34 with vehicle (○) or two different doses of RPI-1, 50 mg/kg (▲) and 100 mg/kg (●). **B**) TT tumor-bearing mice were treated for 40 days with vehicle (○) or 100 mg/kg RPI-1 (●) from day 27 to day 66. Each point represents the mean tumor weight from 8–10 mice. **Error bars** represent the 95% confidence intervals. **Arrows** indicate the beginning and the end of RPI-1 treatment. Statistical significance of the difference between tumor weights measured in RPI-1-treated versus control mice was calculated with the two-sided Student's *t* test at the days of maximum tumor weight inhibition (as reported in Table 2) and at days 53 (**A**) or 110 (**B**). *$P = .01$, †$P = .003$, ‡$P < .001$.

were statistically significantly lower in treated mice than in control mice ($P = .01$, by Student's t test).

Discussion

This study shows that Ret receptors carrying activating mutations at C634 characteristic of the MEN2A syndrome are targets of the 2-indolinone compound RPI-1. Inhibition of Ret tyrosine phosphorylation was associated with a decrease in Ret expression both in RET^{C634R}-transfected NIH3T3 cells and in the TT human medullary thyroid carcinoma cell line harboring the RET^{C634W} mutant. In addition, these results are, to our knowledge, the first demonstration of a marked growth inhibition of human medullary thyroid carcinoma xenografts (harboring a MEN2A-type RET mutation) achieved by oral treatment with a well-tolerated Ret inhibitor. Therefore, RPI-1 might have potential therapeutic applications similar to those of Gleevec [a well-known, clinically useful tyrosine kinase inhibitor *(32)*] in solid tumors harboring pathologically relevant mutated tyrosine kinases.

The clinical relevance of RET in papillary and medullary thyroid cancers has been recognized for many years *(6)* and has recently been supported by the observation that transgenic mice expressing RET oncogenes develop thyroid tumors *(8,9)*. Thus, the involvement of the RET proto-oncogene in the molecular pathology of thyroid cancers provided a rational basis to investigate the role of Ret tyrosine kinases as therapeutic targets. Our previous studies demonstrated that RPI-1 inhibits the tyrosine kinase activity of the Ret/ptc1 oncoprotein and selectively arrests the growth of either NIH3T3 transfectants carrying the Ret/ptc1 oncoprotein or a papillary thyroid carcinoma cell line spontaneously expressing the RET/PTC1 rearrangement *(18,19)*. Similar results have been obtained by others with structurally different tyrosine kinase inhibitors such as the pyrazolo pyrimidines PP1 and PP2 *(33,34)* and the quinazoline ZD6474 *(35)*. These studies suggested the possibility of using Ret inhibitors to treat tumors carrying Ret abnormalities including medullary thyroid carcinoma, a more aggressive disease than papillary thyroid carcinoma with a poor responsiveness to conventional chemotherapy. In the present study, the *in vitro* experiments demonstrated that RPI-1 concentrations that inhibit Ret tyrosine autophosphorylation and signaling have antiproliferative activity on cells expressing ectopic and endogenous MEN2A-type RET mutants ($NIH3T3^{MEN2A}$ transfectants and TT cells), supporting the hypothesis that RPI-1 may have therapeutic potential in the treatment of patients with medullary thyroid carcinomas carrying MEN2A-type mutations.

An interesting feature shared by RPI-1 and the two pyrazolo pyrimidines PP1 and PP2 is the ability to specifically lower the expression of mutant RET^{C634} receptors [*(20)* and Figs. 1, A, and 3, A]. The molecular mechanism by which RPI-1 lowers Ret expression is not yet known. The inhibitory effect of PP1 on receptor expression has been ascribed to stimulation of the proteasome-mediated degradative pathway *(20)*. Other tyrosine kinase inhibitors have recently been described as activating a chaperone-mediated pathway that targets ErbB2 for intracellular degradation *(36)*. Together, these observations suggest that the therapeutic efficacy of tyrosine kinase inhibitors might be attributed also to their ability to reduce expression of oncoproteins. A better knowledge of the mechanisms that regulate oncoprotein activity and expression will provide the basis for devising more specific strategies to inhibit them.

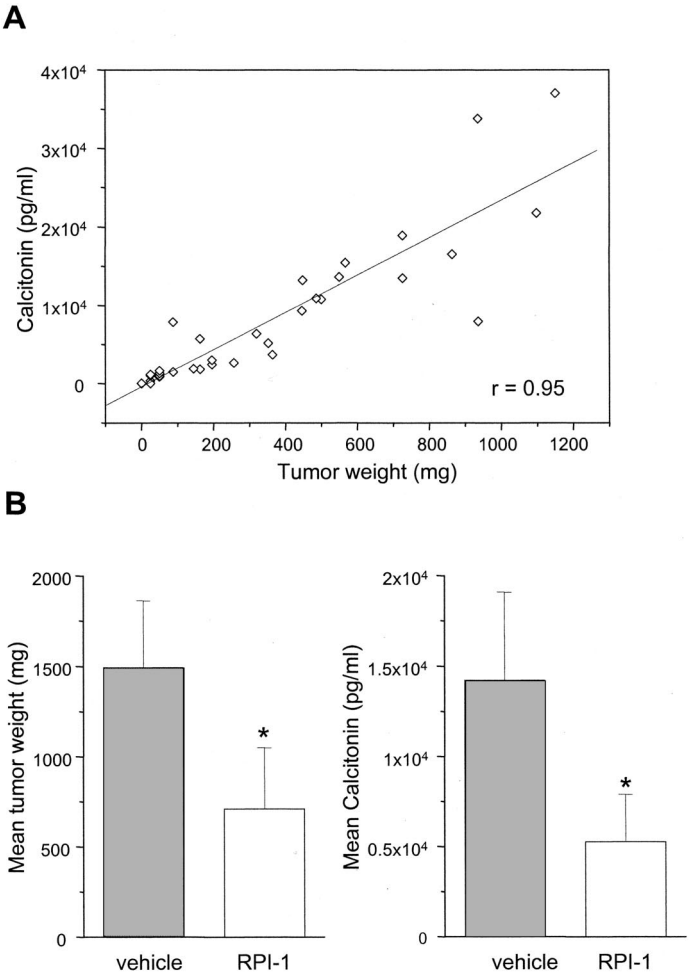

Fig. 5. Effects of RPI-1 treatment on calcitonin plasma levels in human TT tumor-bearing mice. **A**) Linear relationship between tumor weight and calcitonin plasma levels. Blood from control and treated mice was collected at different times during the experiments reported in Fig. 4. Plasma calcitonin concentration was measured using an immunoradiometric assay, and the concentrations were plotted against the respective tumor weight ($r = .95$ and $P<.001$ by Spearman rank correlation test). **B**) Calcitonin plasma levels in TT tumor-bearing mice. Mice were treated orally twice daily with RPI-1 at a dose of 100 mg/kg for 40 days (experiment reported in Fig. 4, B). At day 110, tumor weights were measured, and blood was collected for plasma calcitonin measurement. Data represent the mean values obtained from eight mice per group. **Error bars** indicate the upper 95% confidence interval. Statistical significance of RPI-1-treated (**open columns**) versus control (**solid columns**) mice was assessed by two-sided Student's t test (*$P = .01$).

The molecular basis of the inhibitory effects of RPI-1 was supported by the results of experiments designed to examine Ret-dependent signaling in the presence and absence of RPI-1. RPI-1 blocked Ret-dependent signaling in our experimental model. Specifically, Ret did not bind to PLCγ, and overall, PLCγ was inactive in RPI-1-treated TT cells. Similar results were obtained in papillary thyroid carcinoma cells expressing Ret/ptc1 *(19)*. The interaction of Ret/ptc2 or of Ret/ptc1 with PLCγ through pY1015 has been shown to be required for full oncogenic activation *(24)* and for thyroid tumor formation in transgenic mice *(37)*. The precise definition of the role of PLCγ in the signaling of receptor Ret oncoproteins is needed to clarify the biologic consequences of its inhibition. Our findings also

showed that Ret inactivation by RPI-1 was associated with inhibition of AKT- and ERK-dependent pathways in TT cells, which supports the previous finding that the transforming ability of the MEN2A Ret mutant requires activation of the PI3K/AKT signaling pathway *(30)*. Indeed, our data support the finding that the pY1062 Ret docking site is essential for the activation of both pathways *(38)*, because pY1062 phosphorylation disappeared following the same dose-dependent, drug-induced AKT and ERK dephosphorylation in our experimental model. Although we cannot exclude the possibility that the inhibition of additional receptor tyrosine kinases by RPI-1 might contribute to the inhibition of downstream pathways, as reported for other inhibitors of the indolinone series *(39)*, our results suggest that the inhibition of Ret has a strong effect on cellular signal transduction pathways.

The most relevant result of our study was the strong and reproducible antitumor activity of RPI-1 against the human medullary thyroid carcinoma TT xenograft in nude mice. Tumor growth inhibition was dose- and time-dependent, and optimal effects were observed after prolonged daily treatment. Importantly, the compound was delivered orally, the most suitable delivery route for prolonged treatment. The low solubility of RPI-1 did not allow us to establish a maximum tolerated dose in mice. However, a strong antitumor effect was achieved by a well-tolerated dose (100 mg/kg of body weight). At this RPI-1 dose, 25% of treated mice were tumor-free at the end of the experiments. The antitumor effect was obtained in spite of the relatively low oral bioavailability of the drug in the current formulation, as found in preliminary pharmacokinetic studies. Therefore, detailed *in vivo* studies will be necessary to define the optimal treatment conditions to fully exploit the therapeutic potential of the drug.

Several clinical studies have addressed the problem of identifying the maximum tolerated dose in the development of "target-oriented drugs," including tyrosine kinase inhibitors *(40,41)*. Data from phase II clinical trials with Gleevec revealed that it was possible to identify a "biologically active dose" lower than the maximum tolerated dose assessed in a typical phase I study *(42)*. For the clinical development of tyrosine kinase inhibitors, determination of pharmacodynamic parameters should allow optimization of the therapy. Our study indicated that plasma calcitonin levels effectively reflect the TT tumor response to RPI-1 treatment. Thus, the plasma calcitonin level, which is recognized as a specific and sensitive medullary thyroid carcinoma marker, might be a useful tool for measuring RPI-1 efficacy in clinical trials.

In conclusion, our studies indicate that Ret oncoproteins represent exploitable therapeutic targets in MEN2A-associated medullary thyroid carcinoma and have the potential to provide a new option for the treatment of RET oncogene-related thyroid carcinomas. Because of its ability to inhibit tumor growth at nontoxic doses and its oral bioavailability, the 2-indolinone RPI-1 is a Ret inhibitor of particular pharmacologic interest.

REFERENCES

(1) Fraker DL, Skarulis M, Livolsi V. Thyroid tumors. In: DeVita VT Jr, Hellman S, Rosenberg SA, editors. Cancer: principles and practice of oncology. 6th ed. Philadelphia (PA): Lippincott; 2001. p. 1740–62.

(2) Lairmore TC, Wells SA, Moley JF. Molecular biology of endocrine tumors. In: DeVita VT Jr, Hellman S, Rosenberg SA, editors. Cancer: principles and practice of oncology. 6th ed. Philadelphia (PA): Lippincott; 2001. p. 1727–40.

(3) Cohen MS, Moley JF. Surgical treatment of medullary thyroid carcinoma. J Internal Med 2003;253:616–26.

(4) Wells SA, Franz C. Medullary carcinoma of the thyroid gland. World J Surg 2000;24:952–6.

(5) Bongarzone I, Pierotti MA, Monzini N, Mondellini P, Manenti G, Donghi R, et al. High frequency of activation of tyrosine kinase oncogenes in human papillary thyroid carcinoma. Oncogene 1989;4:1457–62.

(6) Jhiang SM. The RET proto-oncogene in human cancer. Oncogene 2000; 19:5590–7.

(7) Ponder BA, Smith D. The MEN II syndromes and the role of the ret proto-oncogene. Adv Cancer Res 1996;70:179–222.

(8) Michiels FM, Chappuis S, Caillou B, Pasini A, Talbot M, Monier R, et al. Development of medullary thyroid carcinoma in transgenic mice expressing the RET protooncogene altered by a multiple endocrine neoplasia type 2A mutation. Proc Natl Acad Sci U S A 1997;94:3330–5.

(9) Acton DS, Velthuyzen D, Lips CJ, Hoppener JW. Multiple endocrine neoplasia type 2B mutation in human RET oncogene induces medullary thyroid carcinoma in transgenic mice. Oncogene 2000;19:3121–5.

(10) Takahashi M. The GDNF/RET signaling pathway and human diseases. Cytokine Growth Factor Rev 2001;12:361–73.

(11) Takahashi M, Buma Y, Taniguchi M. Identification of the ret proto-oncogene products in neuroblastoma and leukaemia cells. Oncogene 1991; 6:297–301.

(12) Chappuis-Flament S, Pasini A, De Vita G, Segouffin-Cariou C, Fusco A, Attie T, et al. Dual effect on RET receptor of MEN 2 mutations affecting specific extracytoplasmic cysteines. Oncogene 1998;17:2851–61.

(13) Ito S, Iwashita T, Asai N, Murakami H, Iwata Y, Sobue G, et al. Biological properties of Ret with cysteine mutations correlate with multiples endocrine neoplasia type 2A, familial medullary thyroid carcinoma, and Hirschsprung's disease phenotype. Cancer Res 1997;57:2870–2.

(14) Iwashita T, Kato M, Murakami H, Asai N, Ishiguro Y, Ito S, et al. Biological and biochemical properties of Ret with kinase domain mutations identified in multiple endocrine neoplasia type 2B and familial medullary thyroid carcinoma. Oncogene 1999;18:3919–22.

(15) Lanzi C, Borrello MG, Bongarzone I, Migliazza A, Fusco A, Grieco M, et al. Identification of the product of two oncogenic rearranged forms of the RET proto-oncogene in papillary thyroid carcinomas. Oncogene 1992;7: 2189–94.

(16) Hansford JR, Mulligan LM. Multiple endocrine neoplasia type 2 and RET: from neoplasia to neurogenesis. J Med Genet 2000;37:817–27.

(17) Shawver LK, Slamon D, Ullrich A. Smart drugs: tyrosine kinase inhibitors in cancer therapy. Cancer Cell 2002;1:117–23.

(18) Lanzi C, Cassinelli G, Pensa T, Cassinis M, Gambetta RA, Borrello MG, et al. Inhibition of transforming activity of ret/ptc1 oncoprotein by a 2-indolinone derivative. Int J Cancer 2000;85:384–90.

(19) Lanzi C, Cassinelli G, Cuccuru G, Zaffaroni N, Supino R, Vignati S, et al. Inactivation of Ret/Ptc1 oncoprotein and inhibition of papillary thyroid carcinoma cell proliferation by indolinone RPI-1. Cell Mol Life Sci 2003; 60:1449–59.

(20) Carniti C, Perego C, Mondellini P, Pierotti MA, Bongarzone I. PP1 inhibitor induces degradation of RETMEN2A and RETMEN2B oncoproteins through proteasomal targeting. Cancer Res 2003;63:2234–43.

(21) Borrello MG, Smith DP, Pasini B, Bongarzone I, Greco A, Lorenzo MJ, et al. RET activation by germline MEN2A and MEN2B mutations. Oncogene 1995;11:2419–27.

(22) Carlomagno F, Salvatore D, Santoro M, de Franciscis V, Quadro L, Panariello L, et al. Point mutation of the RET proto-oncogene in the TT human medullary thyroid carcinoma cell line. Biochem Biophys Res Commun 1995;207:1022–8.

(23) Shekan P, Storeng R, Scudiero D, Monks A, McMahon J, Vistica D, et al. New colorimetric cytotoxicity assay for anticancer-drug screening. J Natl Cancer Inst 1990;82:1107–12.

(24) Borrello MG, Alberti L, Arighi E, Bongarzone I, Battistini C, Bardelli A, et al. The full oncogenic activity of Ret/ptc2 depends on tyrosine 539, a docking site for phospholipase Cgamma. Mol Cell Biol 1996;16:2151–63.

(25) Yamamoto M, Li M, Mitsuma N, Ito S, Kato M, Takahashi M, et al. Preserved phosphorylation of RET receptor protein in spinal motor neurons

of patients with amyotrophic lateral sclerosis: an immunohistochemical study by a phosphorylation-specific antibody at tyrosine 1062. Brain Res 2001;912:89–94.
(26) United Kingdom Co-ordinating Committee on Cancer Research (UKCCCR) Guidelines for the Welfare of Animals in Experimental Neoplasia (Second Edition). Br J Cancer 1998;77:1–10.
(27) Armitage P, Berry G. Statistical methods in medical research. 2nd ed. Oxford (U.K.): Blackwell Scientific Publishers; 1987. p. 411–20.
(28) Salvatore D, Barone MV, Salvatore G, Melillo RM, Chiappetta G, Mineo A, et al. Tyrosines 1015 and 1062 are in vivo autophosphorylation sites in Ret and Ret-derived oncoproteins. J Clin Endocrinol Metab 2000;85:3898–907.
(29) Asai N, Murakami H, Iwashita T, Takahashi M. A mutation at tyrosine 1062 in MEN2A-Ret and MEN2B-Ret impairs their transforming activity and association with shc adaptor proteins. J Biol Chem 1996;271:17644–9.
(30) Segouffin-Cariou C, Billaud M. Transforming ability of MEN2A-RET requires activation of the phosphatidylinositol 3-kinase/AKT signaling pathway. J Biol Chem 2000;275:3568–76.
(31) Besset V, Scott RP, Ibanez CF. Signaling complexes and protein-protein interactions involved in the activation of the Ras and phosphatidylinositol 3-kinase pathways by the c-Ret receptor tyrosine kinase. J Biol Chem 2000;275:39159–66.
(32) Druker BJ. STI571 (Gleevec) as a paradigm for cancer therapy. Trends Mol Med 2002;8(4 Suppl):S14–8.
(33) Carlomagno F, Vitagliano D, Guida T, Napolitano M, Vecchio G, Fusco A, et al. The kinase inhibitor PP1 blocks tumorigenesis induced by RET oncogenes. Cancer Res 2002;62:1077–82.
(34) Carlomagno F, Vitagliano D, Guida T, Basolo F, Castellone MD, Melillo RM, et al. Efficient inhibition of RET/papillary thyroid carcinoma oncogenic kinases by 4-amino-5-(4-chloro-phenyl)-7-(t-butyl)pyrazolo[3,4-d]pyrimidine (PP2). J Clin Endocrinol Metab 2003;88:1897–902.
(35) Carlomagno F, Vitagliano D, Guida T, Ciardiello F, Tortora G, Vecchio G, et al. ZD6474, an orally available inhibitor of KDR tyrosine kinase activity, efficiently blocks oncogenic RET kinases. Cancer Res 2002; 62:7284–90.
(36) Citri A, Alroy I, Lavi S, Rubin C, Xu W, Grammatikakis N, et al. Drug-induced ubiquitylation and degradation of ErbB receptor tyrosine kinases: implications for cancer therapy. EMBO J 2002;21:2407–17.
(37) Buckwalter TL, Venkateswaran A, Lavender M, La Perle KM, Cho JY, Robinson ML, et al. The roles of phosphotyrosines-294, -404, and -451 in RET/PTC1-induced thyroid tumor formation. Oncogene 2002;21:8166–72.
(38) Hayashi H, Ichihara M, Iwashita T, Murakami H, Shimono Y, Kawai K, et al. Characterization of intracellular signals via tyrosine 1062 in RET activated by glial cell line-derived neurotrophic factor. Oncogene 2000;19:4469–75.
(39) Mendel DB, Laird AD, Xin X, Louie SG, Christensen JG, Li G, et al. In vivo antitumor activity of SU11248, a novel tyrosine kinase inhibitor targeting vascular endothelial growth factor and platelet-derived growth factor receptors: determination of a pharmacokinetic/pharmacodynamic relationship. Clin Cancer Res 2003;9:327–37.
(40) Korn EL, Arbuck SG, Pluda JM, Simon R, Kaplan RS, Christian MC. Clinical trial designs for cytostatic agents: are new approaches needed? J Clin Oncol 2001;19:265–72.
(41) Baselga J. Skin as a surrogate tissue for pharmacodynamic end points: is it deep enough? Clin Cancer Res 2003;9:2389–90.
(42) Mauro MJ, O'Dwyer M, Heinrich MC, Druker BJ. STI571: a paradigm of new agents for cancer therapeutics. J Clin Oncol 2002;20:325–34.

NOTES

Supported in part by Ministero della Sanità, Ministero Istruzione Università e Ricerca (Fondo per gli Investimenti della Ricerca di Base [FIRB] project), Associazione Italiana per la Ricerca sul Cancro and the Fondazione Thomas Hoepli. G. Cuccuru was supported by a fellowship from the Fondazione Italiana per la Ricerca sul Cancro (FIRC).

We thank Marco A. Pierotti for encouragement and involvement in this research project, the Medicinal Chemistry Department of Novuspharma S.p.A., now Cell Therapeutics, Inc., Europe (Bresso, Italy) for the synthesis of RPI-1, Italia Bongarzone and Maria G. Borrello for discussion and providing the cell lines and the anti-Ret antibody used in this study, Masahiko Yamamoto for providing the anti-p1062-Ret antibody, and Laura Zanesi for help in editing the text.

Manuscript received September 29, 2003; revised April 26, 2004; accepted May 14, 2004.